Journal of Structural Geology, Vol. 11, No. 7, pp. 919 to 931, 1989
Printed in Great Britain

0191-8141/89 $03.00 + 0.00

The thermal response of rock to friction in the drag cutting process

DAVID A. GLOWKA

Geothermal Research Division, Sandia National Laboratories, Albuquerque, NM 87185, U.S.A.

(*Received* 26 *August* 1988; *accepted in revised form* 9 *May* 1989)

Abstract—Significant friction between the cutter and the rock occurs during the drag cutting process. This friction is responsible for elevating the temperature of the drag cutter and, under certain conditions, reducing cutter life. Because of this effect, friction often plays a major role in determining the economics of drilling with drill bits employing polycrystalline diamond compact (PDC) cutters. Analytical models have been developed in previous studies for predicting PDC cutter temperatures and their effects on bit wear and performance.

The current paper investigates the effects of drag cutter friction on the rock mass and on rock chips generated during cutting. The thermal and mechanical loading imposed during the cutting process is described, and the thermal response of the rock to frictional heating at the cutter–rock interface is investigated. The results indicate that significant localized rock temperatures can develop as a result of frictional heating caused by drag cutters sliding on the rock surface. Although conduction of heat is severely limited during the short chip formation process, it is possible to attain elevated temperatures throughout a rock chip because of the possibility of internal frictional heating caused by shear deformation. It is concluded that temperatures and pressure during drag cutting are sufficient to cause 'metamorphic' changes in some rock constituents.

NOMENCLATURE

A_w	cutter wearflat area in contact with the rock (cm^2)
C_1	penetrating force correlation constant for sharp cutters (N/cm^{n1})
C_2	penetrating stress correlation constant for worn cutters (MPa/cm^{n2})
D	dimensionless wearflat length (equation 13c)
f	cutter thermal response function (°C/W-cm^2)
F	cutter penetrating force (N)
F_c	cutting force (N)
F_d	cutter drag force (N)
F_f	cutter–rock friction force (N)
k	rock thermal conductivity (W/cm-°C)
K_0	modified Bessel function of the second kind of order zero
L	cutter wearflat length parallel to cutting direction (cm)
L_h	length of hole drilled (m)
$n1$	penetrating force correlation exponent for sharp cutters
$n2$	penetrating stress correlation exponent for worn cutters
N	bit rotary speed (rev/min)
q_c	frictional heat flux into cutter (W/cm^2)
q_r	frictional heat flux into rock (W/cm^2)
Q	rate of generation of frictional heat (W)
R	cutter radial position on bit (cm)
S_c	compressive rock strength (MPa)
T_D	dimensionless temperature rise in rock
T_f	initial formation and downhole fluid temperatures (°C)
$\bar{T}_r$	mean rock temperature over cutter–rock contact area (°C)
$\bar{T}_w$	mean cutter wearflat temperature over cutter–rock contact area (°C)
V	cutter speed (cm/sec)
w	cutter wearflat width perpendicular to cutting direction (cm)
w_c	width of cut (cm)
x	distance parallel to rock surface and perpendicular to cutting direction (cm)
y	distance parallel to rock surface and cutting direction (cm)
Y	dimensionless y (equation 13d)
z	distance into rock perpendicular to surface and cutting direction (cm)
Z	dimensionless z (equation 13e)
$z_{10\%}$	distance below rock surface at which rock temperature rise is 10% of temperature rise at surface
α	energy partitioning fraction
δ	depth of cut (cm)
δ_e	effective depth of cut (cm)
$\Delta(x)$	local height of rock surface above cutter wearflat (cm)
η	cutter–rock friction coefficient = F_f/F
η_d	cutter drag coefficient = F_d/F
χ	rock thermal diffusivity (cm^2/sec)

INTRODUCTION

THE drag cutting process has long been used as a technique for mining and drilling rocks. Mechanical miners employing drag cutters have been used successfully worldwide to excavate nearly all types of rock for a wide variety of applications. Before the invention of the roller cone bit, drag bits of the fish-tail design were used in petroleum drilling, but they were limited by wear in all but the softest of rocks. In the past decade, more wear-resistant drag bits employing polycrystalline diamond compact (PDC) cutters have experienced a tremendous increase in use in both the mining and drilling industries. In appropriate rock formations, PDC bits are capable of drilling faster and longer than roller bits, resulting in significant savings in drilling costs.

For example, rock penetration rates with PDC bits are often at least twice those achievable with roller bits (e.g. Slack 1981, Keller & Crow 1983, Offenbacher *et al.* 1983). Ten-fold increases in bit life have been reported (Offenbacher *et al.* 1983), with the record PDC bit life reported in the literature now standing at over 6100 m (Gill & Martin 1985). Total drilling cost savings of 30–50% are common with PDC bits in some formations, and savings of more than $100,000 (U.S.) have been reported for a single bit run (Offenbacher *et al.* 1983).

A variety of PDC bits is shown in Fig. 1(a). Note that variables in the bit design include the size and shape of the bit head, the number, size and placement of cutters, and the number, size and location of fluid ports for cleaning and cooling the bit.

A typical PDC cutter is shown in Fig. 1(b). The thin, black layer of material on the leading face of the cutter is the artificial-diamond compact, which provides the wear resistance that makes this type of cutter effective in drilling rock. Randomly oriented, artificial-diamond crystals are bonded together on a tungsten carbide–cobalt (WC–Co) substrate under high temperature and

high pressure in the presence of a catalytic binder (mostly cobalt) (Hibbs & Wentorf 1974, Hibbs & Lee 1978). The random orientation of the diamond crystals retards the growth of microfractures in the structure, thereby providing greater abrasive wear resistance than natural, single-crystal diamonds. The WC–Co substrate supports the polycrystalline diamond layer and absorbs much of the shock transmitted from the rock to the cutter during operation.

The WC–Co substrates with their PDC layers are mounted (usually brazed) to cylindrical WC–Co studs, which in turn are pressed into holes machined into the head of the drill bit. The angle of the stud flat to which the substrate is mounted defines the backrake angle of the cutter relative to the rock. The backrake angle varies from 5 to 20° in most cases, with the larger angles being optimal for hard rock. In some bit designs, the cutters are 'matrix-mounted', in which case the WC–Co substrates are brazed directly onto angled flats cast onto the head of the WC–Co bit.

Numerous fluid ports or nozzles are generally distributed across the face of PDC bits. The size, location and orientation of the ports are important factors in determining the efficiency of the design in cleaning and cooling the cutters (Glowka 1983). Experimentally determined flow patterns across the face of a typical PDC bit are shown in Fig. 2.

More recent experimental work indicates that moderate-pressure (10–30 MPa) waterjets directed at the cutter–rock interface (Fig. 3) are effective in reducing cutting forces (Tutluoglu & Hood 1985, Glowka 1986). Bit designs exploiting this phenomenon could theoretically drill harder rock more effectively than present PDC bit designs (Glowka 1985a, 1987),

In practice, PDC bits are rotated at speeds varying from 60 to 1000 rev/min. In soft-rock drilling with

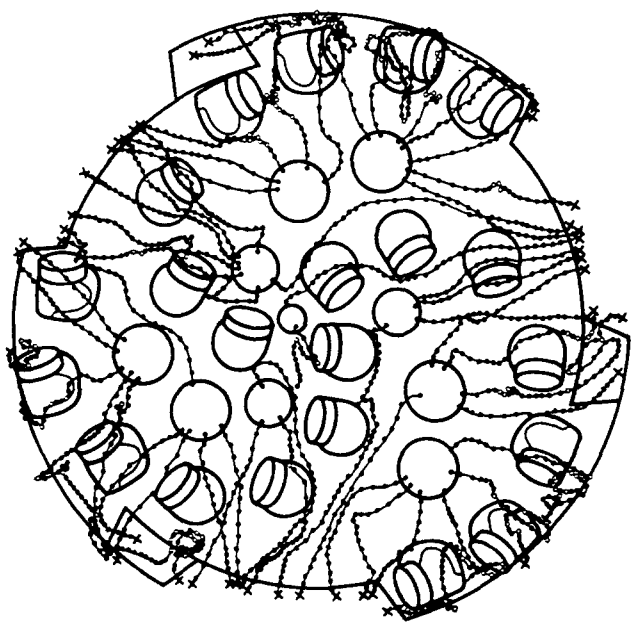

Fig. 2. Flow patterns across the face of a 16.5 cm (6.5 inch) PDC bit as experimentally defined in Glowka (1983). Open symbols correspond to regions of near-zero velocity, as determined from high-speed motion photographs of tracer particle motion.

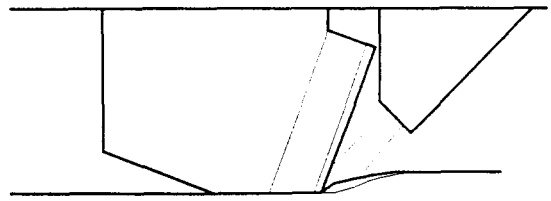

Fig. 3. Concept for providing waterjet assistance to a PDC cutter to reduce cutting forces. Compare with Fig. 2.

downhole motors, speeds in the upper part of this range are successful in yielding economic bit runs (van Proyen *et al.* 1982). In medium-hard rocks, wear rates at high rotary speeds can become significant, so most drilling is done at the lower speeds. Previous analysis shows that bit life is maximized when the ratio of penetration rate to rotary speed is maximized (Glowka 1985b).

Our previous work (see the various Glowka and Glowka & Stone references) concentrated on the drag cutting process as it affects the PDC cutter. In this paper, the primary emphasis is on the cutting process from the standpoint of the rock. After a brief description of the thermal and mechanical loading effects on the cutter, the effects of this loading on the rock are investigated. Although this study generally assumes PDC cutters, the findings are qualitatively applicable to cutting with all types of drag cutters.

PDC CUTTER WEAR CHARACTERISTICS

As drag cutters, PDC cutters slide directly against the rock surface during operation. This action causes both abrasive wear and the generation of significant frictional heat. The rate of abrasive wear is a function of the inherent abrasiveness of the rock, the contact forces between the cutter and the rock, and the temperature of the cutter wearflat (Glowka & Stone 1985, Glowka 1985b). Because of a 'symbiotic' wear relationship between the diamond layer and the WC–Co substrate, the wear characteristics of the PDC cutter are rather complex.

In soft rock with low quartz content, the cutter is subjected to relatively low contact stresses against the rock, and the difference in wear resistance between the diamond and the WC–Co becomes quite evident (Glowka & Stone 1986, Glowka 1987). The WC–Co wears at a higher rate than the thin diamond layer, causing the WC–Co portion of the wearflat to develop at an angle of 5–10° with respect to the rock surface, as shown in Fig. 4. Because of this self-sharpening effect, the wearflat area in contact with the rock is primarily composed of diamond, and the cutting forces are relatively low. The overall cutter wear rate in this soft-rock wear mode is primarily controlled by the abrasive wear resistance of the polycrystalline diamond layer.

In hard rock with high quartz content, however, impact loading on the diamond cutting edge is prevalent as it collides with quartz particles embedded in the rock surface. The shock may be sufficient to break any portion of the cutting edge not fully supported by the

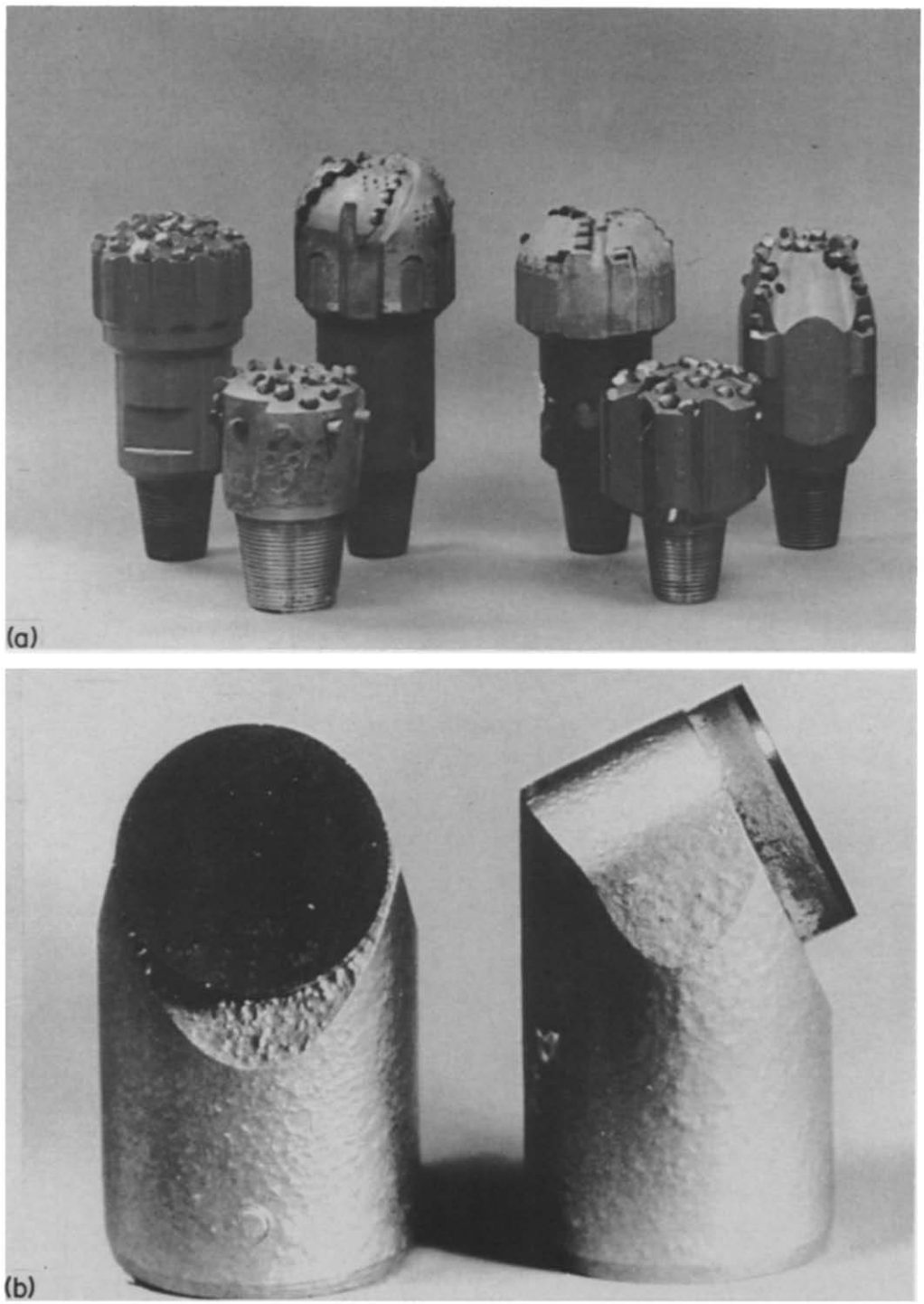

Fig. 1. (a) Collection of 21.6 cm (8.5 inch) PDC drill bits, showing variations in bit shape and location and number of cutters. (b) Single stud-mounted PDC cutter, showing front and side views. The circular diamond face is 1.27 cm (0.5 inch) in diameter.

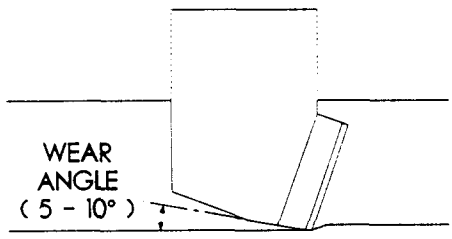

Fig. 4. Wear angle found to develop when cutting soft rock.

WC–Co substrate. As a result, the diamond tends to wear at the same rate as the WC–Co substrate, leading to a wearflat substantially parallel with the rock surface (i.e. wear angle ≈0). The overall cutter wear rate in hard rock is therefore controlled to a large extent by the abrasive wear resistance of the WC–Co substrate. Of course, since the substrate is somewhat protected by the diamond layer from direct impact with protruding quartz particles, the substrate's wear rate in rock is greatly reduced from that of WC–Co alone. Consequently, the abrasive wear resistance of the composite cutter in the hard-rock wear mode is greater than the inherent wear resistance of WC–Co but less than that of polycrystalline diamond.

Regardless of the mode of cutter wear, the wear rate is closely related to the friction between the cutter and the rock. The interference of microscopic asperities between the rock and cutter surfaces is one of the primary contributors to abrasive friction. A similar interference of asperities, but on a wider size scale, is the cause of abrasive wear (Rabinowicz 1965, Glowka & Stone 1986).

Friction at the cutter–rock interface is also responsible for the occurrence of elevated interface temperatures, which play a significant role in determining the wear rate of PDC cutters. At levels below 350°C, the cutter wearflat temperature has very little effect on the cutter wear rate, and abrasive wear proceeds relatively slowly. At temperatures above 350°C, however, PDC cutter wear rates rapidly increase by one to two orders of magnitude, and the cutters quickly become too worn to cut rock effectively (Glowka & Stone 1985, 1986). Since cutter temperatures increase when more weight-on-bit is applied to boost the penetration rate, an upper limit on attainable penetration rate exists, beyond which bit life suffers dramatically (Glowka 1984, 1985a). Because of this effect, friction plays a major role in determining the economics of drilling a given rock formation with PDC drill bits.

The cause of thermally accelerated wear in PDC cutters has been investigated and found to be related to several effects (Glowka & Stone 1986). A primary effect is thermal softening of the WC–Co substrate at temperatures above 350°C. At such elevated temperatures, the hardness of WC–Co degrades to a level comparable to that of quartz particles in the rock, and the abrasive wear rate increases accordingly.

Of equal importance are the internal stresses that arise in the cutter during high-temperature service. Numerical modeling of cutters in various stages of wear has shown that with cooling rates typical of water-based mud drilling, large thermal gradients develop in the cutter under elevated temperatures, as shown in Fig. 5(a) (Glowka & Stone 1986). The resulting differential thermal expansion of various parts of the cutter significantly increases the compressive stresses imposed in the wearflat region. These stresses, shown in the plot of Fig. 5(b), can exceed the compressive strength of the WC–Co substrate under certain conditions. The result is relatively large-scale deformation and initiation of microfractures in the wearflat region. Similar microfractures are created on a smaller scale by localized deformation resulting from the action of abrasive rock particles. Elevated temperatures also tend to place the diamond layer in tension due to the difference in the coefficients of thermal expansion of diamond (2.5×10^{-6}/°C at 300°C) and WC–Co (5.3×10^{-6}/°C at 300°C).

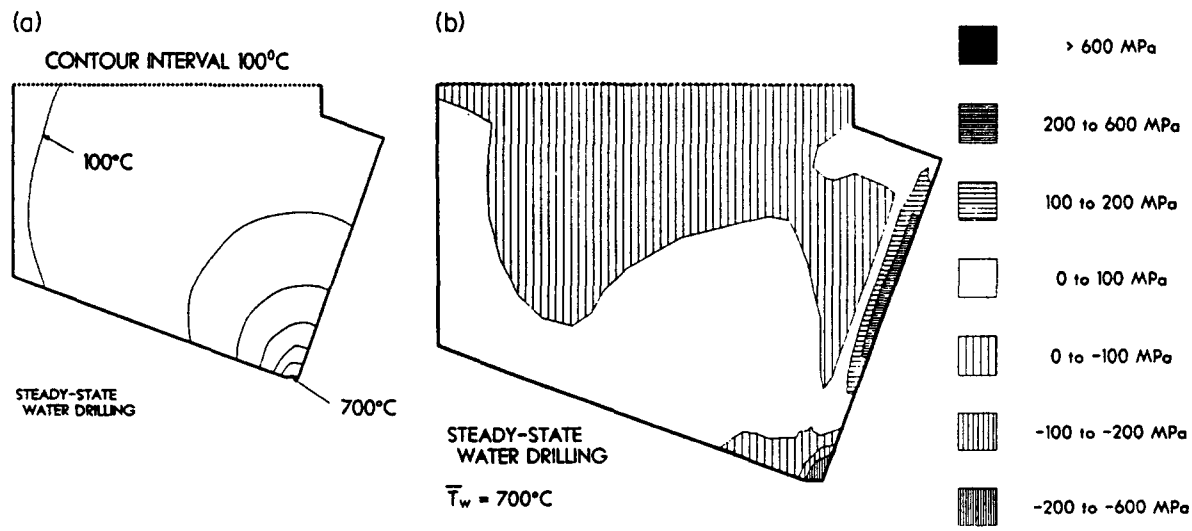

Fig. 5. (a) Calculated PDC cutter temperature field for steady-state water-cooled drilling at an elevated temperature (from Glowka & Stone 1986). (b) Calculated distribution of magnitude of maximum principal stress (compression negative) in a PDC cutter during steady-state water-cooled drilling at an elevated temperature (from Glowka & Stone 1986).

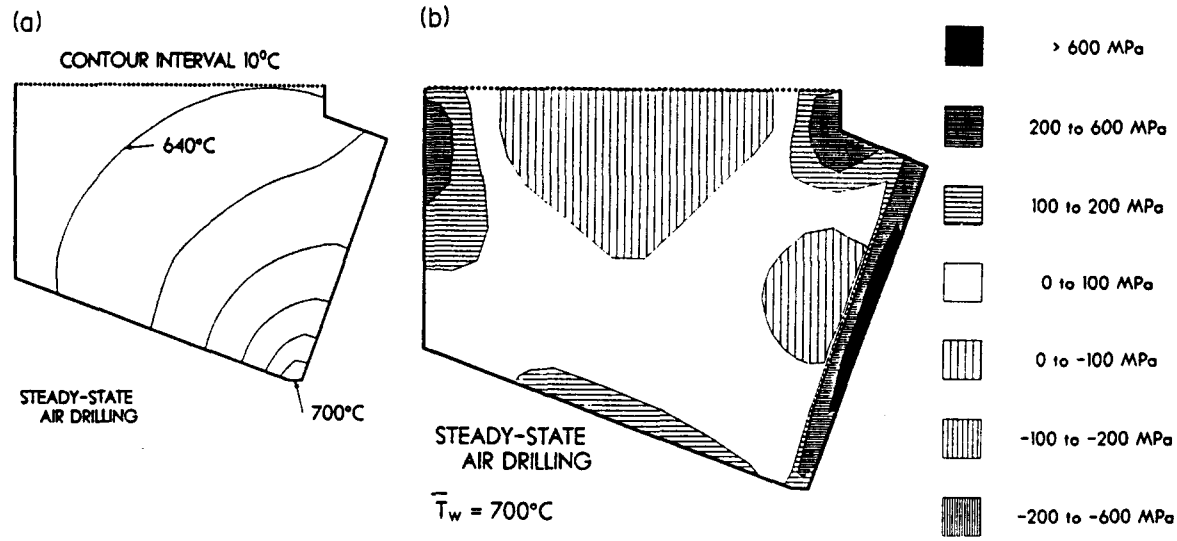

Fig. 6. (a) Calculated PDC cutter temperature field for steady-state air-cooled drilling at an elevated temperature (from Glowka & Stone 1986). (b) Calculated distribution of maximum principal stress magnitude in a PDC cutter during steady-state air-cooled drilling at an elevated temperature (from Glowka & Stone 1986).

Because of poor lubrication and cooling, PDC bits are not often used in air drilling; however, successful runs have been completed in relatively shallow boreholes using compressed air instead of drilling mud (OGJ 1982). Under the relatively poor cooling conditions associated with air drilling, elevated cutter temperatures are attained at much lower cutter forces than those corresponding to mud drilling. As shown in Fig. 6(a), thermal gradients in the cutter are lower, but the entire cutter experiences elevated temperatures. The tendency for differential thermal expansion between the diamond and the WC–Co generates significant tensile stresses along both the diamond face and the wearflat, as shown in Fig. 6(b). These stresses act to propagate microfractures created during the abrasion process, thereby forming wear particles that eventually become evident on a macroscopic scale.

Tensile stresses along the cutter wearflat can also develop under mud-drilling conditions if contact between the cutter and the rock is suddenly lost as a result of bit bounce or the termination of drilling. This effect is illustrated in Fig. 7. Thermal shock caused by rapid cooling reverses the thermal gradients in the wearflat region and changes the stresses from compressive to tensile. This undesirable effect can be eliminated or reduced in two ways: (1) by preventing bit bounce through the use of shock subs in the drill string; and (2) by gradually reducing the weight-on-bit over a period of approximately 30 sec whenever the bit is lifted off-bottom at the termination of drilling (Glowka & Stone 1986).

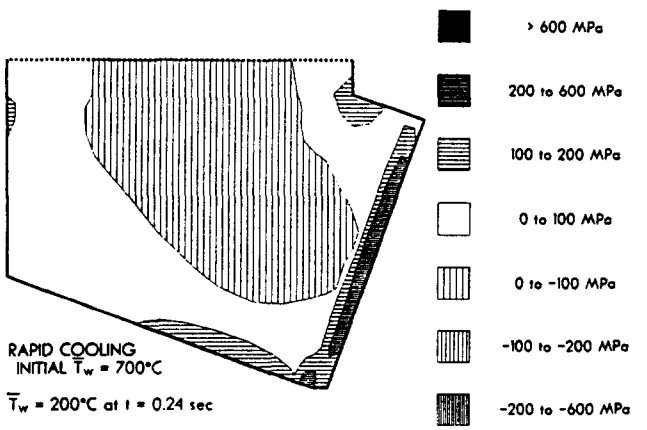

Fig. 7. Calculated distribution of maximum principal stress magnitude in a PDC cutter after breaking contact with the rock surface. Convective cooling of the hot wearflat begins at time $t = 0$ (from Glowka & Stone 1986).

Stresses imposed by the rock on the cutter affect the long-term ability of the cutter to withstand the drilling environment. The effectiveness of the cutter in imposing stresses on the rock, in turn, determines the efficiency of the drilling process.

MECHANICAL ROCK LOADING IMPOSED BY DRAG CUTTING

PDC bits are more efficient in drilling certain formations than either roller bits or natural diamond bits. PDC drag cutters impose tensile and shear stresses in the rock that generally lead to rock chips much larger than those created by the primarily crushing action of teeth on a roller bit. Although natural diamonds also impose drag cutting loads on the rock, each individual diamond cutter is much smaller than a PDC cutter. As a result, rock chips produced by diamond bits are much smaller than those produced by PDC bits and the drilling efficiency is accordingly diminished.

Shown in Fig. 8 is a schematic drawing of the PDC drag cutting process. In making a cut to depth, δ, on a flat rock surface, the cutter imposes the penetrating and drag forces shown in the figure. The penetrating force, F, is related to the weight-on-bit required to penetrate rock at a given rate (Glowka 1987). The drag force, F_d, is the sum of the cutting force, F_c, on the leading edge of the cutter and the friction force, F_f, along the cutter wearflat. The drag force is related to the torque required to rotate the bit during drilling.

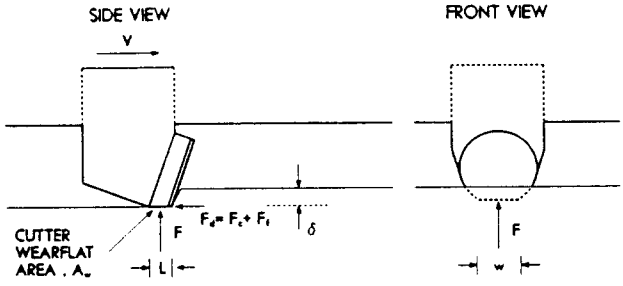

Fig. 8. Schematic drawing of a PDC cutter making a cut to depth, δ, on a flat rock surface.

The penetrating and drag forces are distributed over the cutter wearflat area, A_w, and result in significant compressive, shear and tensile stresses in the rock (Swenson 1983). The effect of those stresses on the rock depends on the operative rock failure mechanism. Hard rock types at low confining pressures tend to fracture in a brittle manner. Experimental study of rock chip morphology, fracture surfaces and subsurface damage in different rock types has suggested that fractures responsible for forming a rock chip are nucleated ahead of the cutter tip, beyond the region of intense compression created by the cutter penetrating force (Zeuch & Finger 1985). These fractures propagate upward to the free surface in a concave downward fashion, as illustrated in Fig. 3. Characteristically large, flat rock chips are formed periodically and are removed from the rock surface by momentum imparted by the sudden release of energy at the fracture surfaces and by the mechanical scavenging action of the drag cutter. Rock chips created in this manner tend to exhibit fractures and crushed zones as artifacts of the chip formation stresses.

In softer rocks, and even hard rocks under elevated confining pressures, more ductile failure apparently occurs (Cheatham & Daniels 1979, Melaugh & Saltzer 1981, Swenson 1983). Fracturing is suppressed, thereby leading to shear stresses that exceed the shear strength of the rock matrix and cause shear deformation. This pseudoplastic failure mechanism can substantially alter the structure of the rock, leaving evidence of plastic flow throughout the rock chips (Taylor 1983, Graves 1986, Spray 1989).

The forces and stresses imposed on the rock surface by PDC cutters have been quantified in previous studies for the purpose of bit design (Glowka 1987). In a given rock type in a given environment, the penetrating force required to cut a flat rock surface with a sharp (new) PDC cutter is related to the depth of cut:

$$F = C_1 \delta^{n1}, \tag{1}$$

where C_1 and $n1$ are defined empirically using the cutter and rock of interest. Results are shown in Fig. 9(a) for a soft rock, Berea sandstone, and a hard rock, Sierra

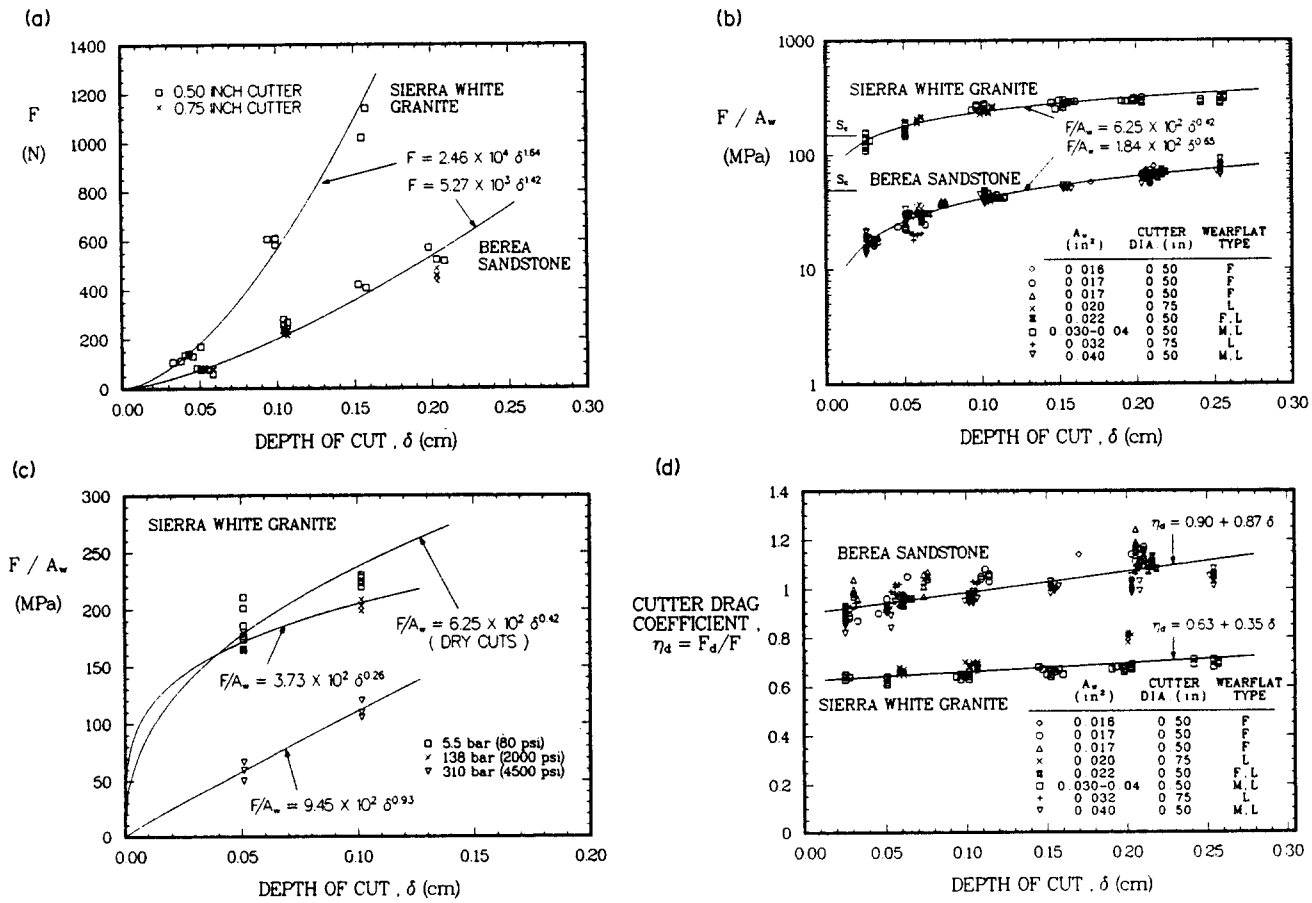

Fig. 9. (a) Measured sharp PDC cutter penetrating forces on a flat rock surface (after Glowka 1987). (b) Measured worn PDC cutter penetrating stresses on a flat rock surface (after Glowka 1987). Wearflat types: F = field-worn in soft rock; L = laboratory-worn in granite; M = machine-ground. (c) Measured worn PDC cutter penetrating stresses with waterjet assistance on a flat rock surface (after Glowka 1987). (d) Measured PDC cutter drag coefficients (after Glowka 1987).

Table 1. Experimental drag cutter force correlation constants

Rock type	S_c (MPa)	C_1 (N/cm^{n1})	$n1$	C_2 (MPa/cm^{n2})	$n2$	η_d
Berea sandstone*	49	5.27×10^3	1.42	1.84×10^2	0.65	0.90
Sierra White granite*	148	2.46×10^4	1.64	6.25×10^2	0.42	0.63
Tennessee marble*	122	—	—	6.92×10^2	0.50	0.65
Norite†	300	—	—	1.33×10^3	0.45	—

* Glowka (1987).
† Glowka (1985b).

White granite. Note that penetrating forces of several hundred Newtons are typical with sharp PDC cutters. Values of C_1 and $n1$ for other rock types are listed in Table 1.

As a cutter wears, it develops a measurable wearflat, A_w, that tends to distribute the penetrating force, thereby reducing the compressive stresses imposed on the rock surface and, consequently, the depth of cut. Under these conditions, the penetrating force is related to the depth of cut in the following manner:

$$F = C_2 A_w \delta^{n2}, \tag{2}$$

where C_2 and $n2$ are determined empirically with a cutter having any measurable wearflat. Results for Berea sandstone and Sierra White granite are shown in Fig. 9(b), and values of C_2 and $n2$ for other rock types are presented in Table 1. The penetrating force increases proportionally with increases in A_w as the cutter wears. With typical wearflat areas for heavily worn PDC cutters being on the order of 0.1–1 cm^2, penetrating forces with worn cutters can range to several thousand Newtons.

Equation (2) indicates that the depth of cut achieved with a drag cutter is a function of the penetrating stress, F/A_w, imposed on the rock surface. Tests with brittle rock indicate that penetrating stresses on the order of the uniaxial compressive rock strength are required before significant penetration of the rock occurs (Glowka 1985a,b, 1987), as with the Sierra White granite shown in Fig. 9(b). This indicates that crushing of the rock surface is necessary to achieve a cut in brittle rock. With more ductile rock types, however, a significant depth of cut is possible at penetrating stress levels well below the compressive strength, as with the Berea sandstone in Fig. 9(b). This indicates that crushing is not as significant to the cutting process when the rock behaves more plastically.

Penetrating stresses measured with waterjet assistance are shown in Fig. 9(c) (Glowka 1987). Note that relatively modest waterjet pressures are capable of significantly reducing cutter penetrating stresses. This reduction is thought to be the result of improved removal of cutting fines, which tend to reduce stresses in the rock by distributing the cutter forces over a large area, and by hydraulic extension of fractures created by the drag cutter.

The drag force may be quantified by use of the equation,

$$F_d = \eta_d F, \tag{3}$$

where η_d is the cutter drag coefficient, an empirically determined constant for a given rock type, cutter type and cutting environment. Results are shown in Fig. 9(d) for Berea sandstone and Sierra White granite. Measured values for other rock types are shown in Table 1. Drag coefficients for ductile rocks are generally of the order of one and tend to be somewhat lower for brittle rocks. Thus the drag component is of greater importance in the drag cutting of ductile rocks than it is in brittle types.

The friction force is related to the penetrating force and the friction coefficient, η, between the cutter and the rock:

$$F_f = \eta F. \tag{4}$$

Measured friction coefficients for various rock types range from 0.03 to 0.33, as shown in Table 2. Note that friction is heavily dependent on the lubricity of the drilling fluid. Water or water-based muds significantly reduce friction from that experienced with dry cutting, such as in air drilling or mining.

The empirical equations presented above were developed using single cutters on smooth rock surfaces. PDC bits used in drilling applications typically have 15–40 cutters per bit. Each cutter takes a unique helical path through the rock as the bit is rotated and advanced to make the hole. Because of the close spacing between cutters, considerable interaction exists among cutters, and the mechanics of the process becomes more complex than those associated with a single cutter.

The effect of cutter interaction is to modify the shape of the rock surface and thus the cross-sectional area of cut for each cutter, as illustrated in Fig. 10. As a result, the forces imposed by the cutter on the rock are modified from those that arise in making a cut on a flat rock surface. A cutter interaction model has been developed

Table 2. PDC cutter–rock friction coefficients (after Glowka & Stone 1985)

Rock type	Cutting speed (m/s)	Friction coefficient		
		Water	Water-based mud	Dry
Marble	1	0.20	0.17	0.33
	5	0.15	0.11	0.15
Sandstone	1	0.03	0.04	0.10
	5	0.05	0.04	0.30
Granite	1	0.09	—	0.18
	5	0.05	—	0.14
Shale	1	0.09	—	0.18
	5	0.06	—	0.15

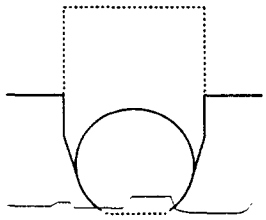

Fig. 10. Typical cutting configuration with cutter interaction, such as occurs with a multiple-cutter bit.

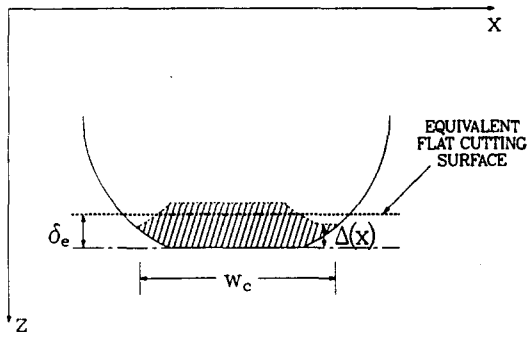

Fig. 11. Definition of effective depth of cut, δ_e, used to predict cutting forces when cutter interaction exists.

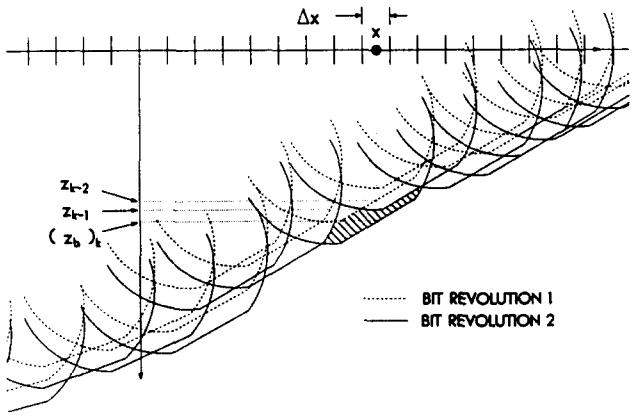

Fig. 12. Schematic diagram of algorithm used to compute effective depth of cut in PDCWEAR bit analysis code (Glowka 1987).

that accounts for these effects (Glowka 1985b, 1986, 1987). In this model, an equivalent flat cutting surface is assumed to exist at the mean elevation of the actual rock surface, as shown in Fig. 11. An effective depth of cut, δ_e, is thus calculated as the mean value of $\Delta(x)$ over the width of the cut. Using this computed value of δ_e in place of δ in equations (1) and (2) allows accurate prediction of the cutting forces that arise during cutter interaction.

This approach is used in a computer code called PDCWEAR that predicts the performance and wear of PDC bits (Glowka 1987). The code allows the user to specify the number, size and location of cutters on the bit body, the shape of the bit and drilling conditions such as bit rotary speed, rock penetration rate and downhole fluid temperature. The program is run interactively, with the user specifying small increments of wear for a reference cutter and the program modifying cutter geometries based on computed relative wear rates. At each wear stage, the program uses the cutter locations and wear configurations to calculate effective depths of cut, cutter forces, temperatures and wear rates. The algorithm used to calculate the effective depths of cut is illustrated in Fig. 12. Cutter forces are also integrated by the program to compute the following bit performance parameters: weight-on-bit, drilling torque, net side force and net bending moment. By evaluating these parameters as a function of bit design, the user can optimize the design for more uniform wear, proper balance, rapid penetration and long life.

THERMAL ROCK LOADING IMPOSED BY DRAG CUTTING

Drag cutting generates frictional heating that can lead to significant cutter and rock temperatures. Energy is converted to heat at the sliding cutter–rock interface, along rock fracture surfaces, and internal to rock chips that undergo shear deformation.

Frictional heating at the cutter–rock interface is a function of the rate at which energy is dissipated by the friction force. The dissipated energy is converted to heat, which is liberated at the rate,

$$Q = F_f V, \tag{5}$$

where V is the cutter speed. A fraction, α, of the frictional heat is assumed to flow into the cutter, with the remaining fraction, $(1-\alpha)$, flowing into the rock. Substituting equation (4) into equation (5) and dividing by the area of contact between the cutter and the rock (A_w) yields equations for the heat flux into the cutter, q_c, and the rock, q_r:

$$q_c = \frac{\alpha \eta F V}{A_w} \tag{6}$$

and

$$q_r = \frac{(1-\alpha)\eta F V}{A_w}. \tag{7}$$

In order to calculate the quantity α, the thermal response of both the rock and the cutter must be known. Jaeger (1942) gives a solution for the mean temperature rise of the contact area between a sliding heat source and a semi-infinite slab as

$$\bar{T}_r - T_f = \frac{4q_r}{3\sqrt{\pi}\,k}\left(\frac{\chi L}{V}\right)^{1/2}, \tag{8}$$

where $\bar{T}_r$ is the mean temperature of the rock surface over the area of contact; T_f is the initial rock formation temperature prior to frictional heating; k is the rock thermal conductivity; χ is the rock thermal diffusivity; and L is the cutter wearflat length parallel to the cutting direction. It is assumed that the initial formation temperature is equal to the fluid temperature, which is also designated T_f. This assumption arises from the vigorous cooling provided to the bottom of the borehole by the drilling fluid.

The thermal response of a PDC cutter to frictional heating is more complex due to the cutter's geometry and composite construction. Thermal numerical modeling of PDC cutters has been conducted (Ortega & Glowka 1984, Glowka & Stone 1985, Glowka 1987), with the results reported in the form,

$$f = \frac{\bar{T}_w - T_f}{q_c}. \tag{9}$$

Here f is defined as the cutter thermal response function, and $\bar{T}_w$ is the mean temperature of the cutter wearflat. Thermal response function values have been computed for several cutter designs and downhole conditions. Factors having the greatest effects on the cutter thermal response were found to be the cutter wearflat length, the cutter cooling coefficient, the thickness of the diamond layer and the thermal conductivity of the WC–Co grade used in the substrate. Typical values of f range from about 0.05 °C/W-cm^2 for mildly worn cutters cooled with water to more than 5°C/W-cm^2 for moderately worn cutters cooled with air.

The pertinent boundary condition at this point in the analysis is the simple assumption that the mean instantaneous temperature of the cutter and the rock along the contact area are equal; i.e.

$$\bar{T}_w = \bar{T}_r. \tag{10}$$

Combining equations (6)–(10), the resulting expression for the energy partitioning fraction, α, is

$$\alpha = \left[1 + \frac{3\sqrt{\pi}\,k}{4}\left(\frac{V}{\chi L}\right)^{1/2} f\right]^{-1}. \tag{11}$$

This equation indicates that as cutting speed V increases, a smaller fraction of the frictional heat flows into the cutter, with a larger fraction consequently flowing into the rock. Other factors that influence this fraction are seen to be the thermal properties of the rock and the computed thermal response of the cutter.

Combining equations (6), (9) and (10) yields an equation for the mean cutter and rock temperature along the wearflat:

$$\bar{T}_r = \bar{T}_w = T_f + \frac{\alpha\eta FV}{A_w} f, \tag{12}$$

where α is determined from equation (11). This equation is used in the PDCWEAR computer code for computing wearflat temperatures (Glowka 1987).

This analysis is extended below to investigate the depth to which the frictional heat penetrates the rock. Another analytical solution of Jaeger (1942) is employed. In equation (7) of his paper, Jaeger gives an expression for the temperature field in a semi-infinite slab as a function of the location (y, z) from the center of a sliding band heat source of infinite extent parallel to the x-axis. In the notation of the present paper, y is the distance parallel to the rock surface and sliding direction; x is the distance parallel to the rock surface and perpendicular to the sliding direction; and z is the distance into the rock perpendicular to the surface and sliding direction. Jaeger gives his solution in terms of a dimensionless temperature rise, defined as

$$T_D \equiv \frac{\pi k V}{2\chi q_r}(\bar{T}_r - T_f). \tag{13a}$$

Jaeger's equation for T_D as a function of location in the rock is

$$T_D(Y,Z) = \int_{Y-D}^{Y+D} e^{-u} K_0(\zeta)\, du, \tag{13b}$$

where

$$D \equiv \frac{VL}{4\chi} \tag{13c}$$

$$Y \equiv \frac{Vy}{2\chi} \tag{13d}$$

$$Z \equiv \frac{Vz}{2\chi} \tag{13e}$$

$$u \equiv \frac{V(y - y')}{2\chi} \tag{13f}$$

and

$$\zeta = \sqrt{Z^2 + u^2}. \tag{13g}$$

Here y' is the distance from the center of the cutter to an arbitrary point on the cutter–rock contact area; and $K_0(\zeta)$ is the modified Bessel function of the second kind of order zero:

$$K_0(\zeta) = \frac{1}{2}\int_0^\infty \frac{1}{\xi} \exp\left[-\frac{1}{2}\zeta\left(\xi + \frac{1}{\xi}\right)\right] d\xi. \tag{13h}$$

Equation (13) can be integrated numerically, as described in the Appendix, to calculate the temperature at any point in the rock. Jaeger shows that this solution is similar to that obtained for a rectangular heat source of finite x-dimension.

To illustrate the use of the rock temperature equations (12) and (13), the PDCWEAR computer code was used to analyze the bit design shown in Fig. 13. This 21.6 cm diameter bit has 21 cutters arranged in a three-

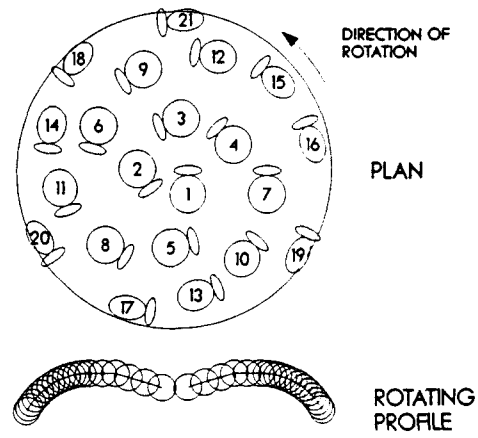

Fig. 13. Bit design used for demonstration purposes in analysis performed using PDCWEAR.

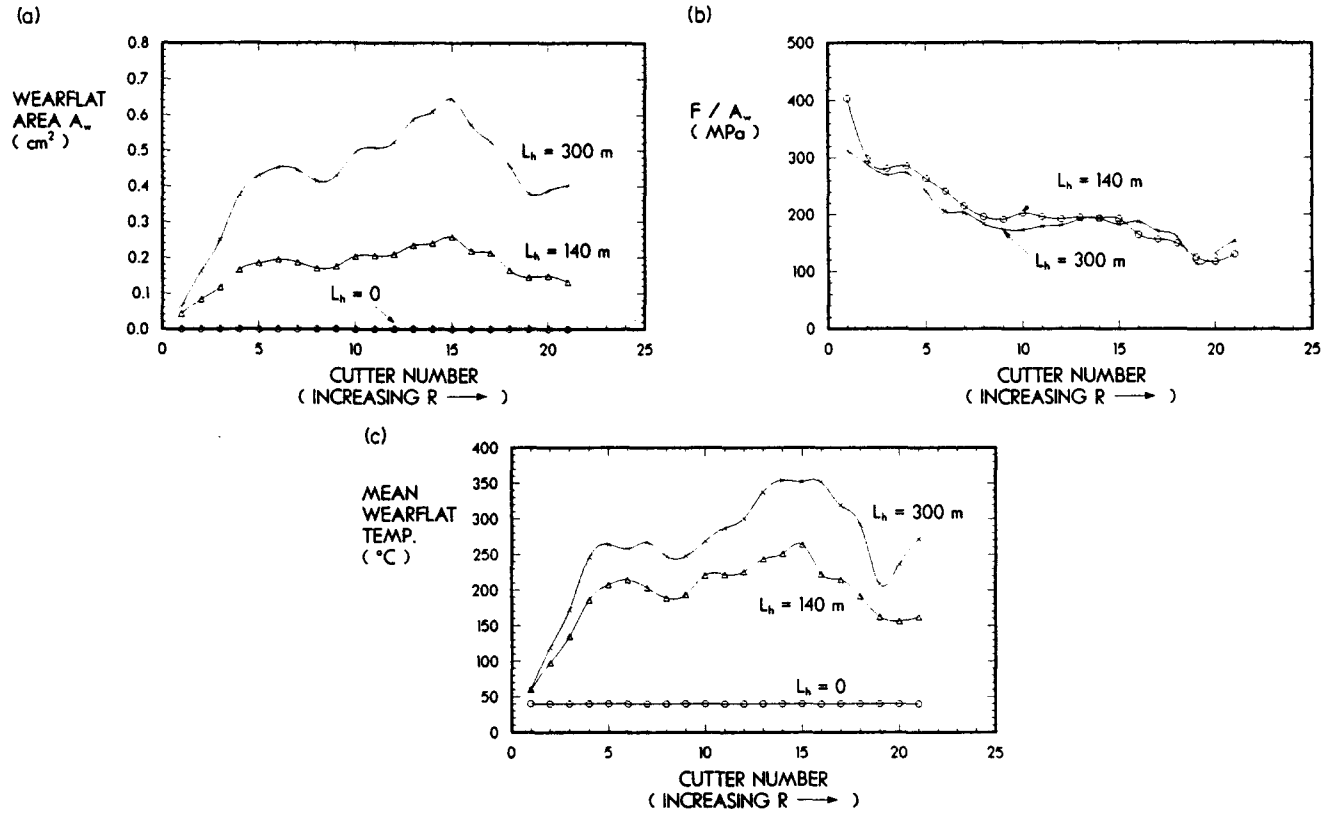

Fig. 14. (a) Predicted cutter wear distribution for demonstration analysis. (b) Predicted penetrating stress distribution for demonstration analysis. (c) Predicted wearflat and rock surface temperature distribution for demonstration analysis.

arm reverse spiral pattern. A generic rock with the strength of Sierra White granite and the abrasiveness of hard sandstone was chosen as a typical rock formation for this analytical bit run. The other selected downhole conditions are presented in Table 3 and include a bit rotary speed of 100 rev/min, a downhole fluid temperature of 40°C and a rock penetration rate of 9.1 m/hr (30 ft/hr). These conditions are typical of PDC bit runs in petroleum drilling.

The results calculated by PDCWEAR are shown in Figs. 14(a)–(c). In Fig. 14(a), the growth in wearflat area is illustrated for each cutter as the hole is drilled. Here L_h represents the length of hole drilled in reaching the corresponding bit wear stages. When the bit is sharp at the beginning of the hole, all wearflat areas are zero, and the predicted weight-on-bit to drill at the selected penetration rate is 15.6 kN. After drilling 300 m, the cutter wear ranges to over 0.6 cm^2, and the required weight-on-bit is calculated to be 146 kN, nearly 10 times that with the sharp bit.

The calculated penetrating stress imposed by each cutter on the rock is shown in Fig. 14(b). Note that stresses of the order of 200 MPa are imposed by most cutters. Variation among the cutters is the result of non-uniform cutter interaction and wear. These stresses would increase in magnitude if the specified bit penetration rate were increased above its specified level for this analysis.

The calculated temperatures at the cutter–rock interface are shown in Fig. 14(c). The temperature attained with each cutter varies according to its wear state, radial position on the bit and interaction with nearby cutters.

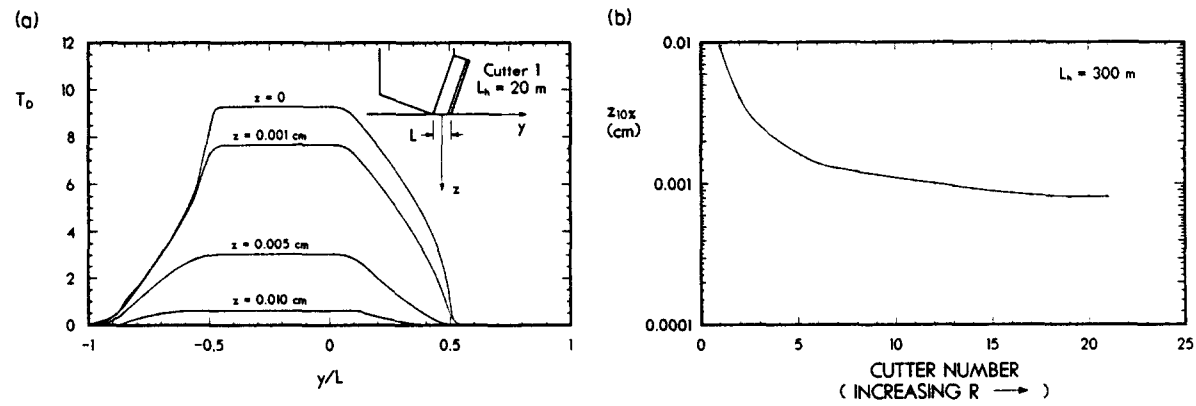

Fig. 15. (a) Dimensionless temperature rise for rock beneath cutter 1 after bit has drilled 20 m in demonstration analysis. (b) Penetration depth of frictional heat into rock surface for demonstration analysis after bit has drilled 300 m. $z_{10\%}$ is the depth at which the rock temperature rise due to frictional heat is 10% of the temperature rise at the rock surface.

Table 3. Bit operating conditions used in demonstration analysis

Parameter	Value
Rock thermal conductivity, k	0.023 W/cm-°C
Rock thermal diffusivity, χ	0.0085 cm^2/sec
Rock–cutter friction coefficient	0.09
Worn cutter drag coefficient	0.55
Sharp cutter drag coefficient	0.75
Sharp cutter correlation constant, C_1	2.46×10^4 N/cm$^{1.64}$
Worn cutter correlation constant, C_2	6.25×10^2 MPa/cm$^{0.42}$
Sharp cutter correlation exponent, $n1$	1.64
Worn cutter correlation exponent, $n2$	0.42
Abrasive wear constant	1.09×10^{-10}/MPa
Bit rotary speed, N	100 rev/min
Downhole cooling fluid temperature, T_f	40°C
Specified bit penetration rate, ROP	9.1 m/s

Note that temperatures above 350°C are attained by three of the cutters after the bit has drilled 300 m. These cutters would be expected to wear at a thermally accelerated rate if further drilling were attempted.

The rock temperature field around cutter 1 after drilling 20 m of hole was calculated as described in the Appendix. The results are presented in Fig. 15(a). Here the dimensionless rock temperature rise, T_D, is plotted as a function of the distance from the center of the cutter wearflat, $(y/L,z)$. (Since the contact area between the cutter and the rock is L, the cutter extends over the range $-0.5 \leq y/L \leq 0.5$ at $z = 0$.) Note that the temperature rise above ambient drops rapidly with distance, z, below the rock surface. At a depth of only 0.01 cm, the temperature rise is less than ten percent of the temperature rise at the rock surface.

This measure of heat penetration is used in Fig. 15(b) to present results for each cutter after the bit has drilled 300 m. Shown here is the rock depth, $z_{10\%}$, below the trailing edge of each cutter at which the temperature rise is 10% of the rock surface temperature rise. Note that as radial position on the bit increases, the cutting speed also increases, resulting in more shallow penetration of frictional heat into the rock. At radial positions where significant wearflat temperatures develop, $z_{10\%}$ is only about 0.001 cm (1/100 mm). Consequently, it can be concluded that any elevated temperatures that develop at the cutter–rock interface due to frictional heating do not penetrate beyond a fraction of a millimeter into the rock surface. Since the depth of cut is generally of the order of 0.1–1 mm, the thermally affected zone that develops in the rock mass during one pass of a cutter is removed with the rock chip created during the next pass of a cutter.

DISCUSSION

Under the assumed conditions of the demonstration analysis, rock surface temperatures remain at or below 350°C, and frictional heat generated at the cutter–rock interface does not penetrate beyond a fraction of a millimeter into the rock surface. These conditions were selected, however, to ensure that the maximum cutter wearflat temperature in the demonstration analysis did not exceed the 350°C limit for normal abrasive wear. Under high-temperature, high-wear conditions resulting, for example, from higher rotary speeds, higher downhole formation temperatures, or higher bit penetration rates, rock surface temperatures can easily exceed the 350°C limit. Furthermore, natural diamonds are thermally stable to temperatures of at least 1200°C; thus rock surface temperatures attained when drilling under normal diamond-bit drilling conditions can be considerably higher than those predicted in the demonstration analysis.

The stresses that develop in rock chips during the chip formation process may also cause intense internal heating, depending on the rock failure mode. If the rock behaves plastically and undergoes significant shear deformation, rock chips will experience significant localized heating caused by internal friction. Because of the high stress magnitude and short time period involved, it is reasonable to expect such internal heating to lead to local, instantaneous temperatures of at least the same magnitude as those calculated for the cutter–rock interface. Indeed, evidence for elevated internal rock chip temperatures has been observed in chips generated by natural diamond drag bits, where alteration textures ranged from polishing of mineral–clast surfaces (slickensiding) through plastic deformation to fusion to form glass (Taylor 1983, Spray 1989). Such alterations have been referred to as 'bit metamorphism' because of the obvious effects of temperature and pressure on mineral composition.

A comparison of recognized metamorphic conditions with conditions that exist during drag cutting supports the idea of 'bit metamorphism'. Pressures experienced by rock chips during drag cutting can reach several hundred MPa, and rock temperatures can reach several hundred degrees Celsius. The pressures and temperatures attained under typical drag-bit drilling conditions are thus well within the range where 'metamorphism' of some rock constituents is possible, although this term may be a misnomer since true rock metamorphism is usually considered to be a relatively slow process. Because of the extremely low transition velocities for most minerals, crystallization experiments studying rock metamorphism typically last several minutes or hours (Sobolev & Dobretsov 1972), whereas the high-temperature, high-pressure history associated with drag cutting is only a fraction of a second long. Regardless of the terminology used, however, it is clear that shear deformation by PDC cutters can lead to structural changes in rock chips created in some formations. Whether or not thermal effects related to the shear deformation will also arise in a given case probably depends on *in situ* conditions, such as mineral composition and formation temperature, as well as bit operating conditions, such as rotary speed, weight-on-bit, lubrication and cooling.

Acknowledgments—This work was performed at Sandia National Laboratories, supported by the U.S. Department of Energy under contract DE-AC04-76DP00789.

REFERENCES

Cheatham, J. B., Jr. & Daniels, W. H. 1979. A study of factors influencing drillability of shales: single cutter experience with Stratapax drill blanks. *J. Energy Resources Technol.* **101**, 189–195.

Gill, C. W. & Martin, J. L. 1985. Matrix body PDC bits prove most cost effective in the Powder River Basin. Paper 13462, 1985 International Association of Drilling Contractors/Society of Petroleum Engineers Drilling Conference, New Orleans, Louisiana, 331–354.

Glowka, D. A. 1983. Optimization of bit hydraulic configurations. *Soc. Petrol. Engrs J.* **23**, 21–32.

Glowka, D. A. 1984. Thermal limitations on the use of PDC bits in geothermal drilling. *Trans. Geothermal Res. Council* **9**, 261–266.

Glowka, D. A. 1985a. Design considerations for a hard-rock PDC drill bit. *Trans. Geothermal Res. Council* **9**, 123–128.

Glowka, D. A. 1985b. Implications of thermal wear phenomena for PDC bit design and operation. Paper 14222, 60th Annual Technology Conference and Exhibition of the Society of Petroleum Engineers, Las Vegas, Nevada.

Glowka, D. A. 1986. The use of single-cutter data in the analysis of PDC bit design and operation. Paper 14222, 61st Annual Technology Conference and Exhibition of the Society of Petroleum Engineers, New Orleans, Louisiana.

Glowka, D. A. 1987. Development of a method for predicting the performance and wear of PDC drill bits. Report SAND86-1745, Sandia National Laboratories, Albuquerque, New Mexico.

Glowka, D. A. & Stone, C. M. 1985. Thermal response of polycrystalline diamond compact cutters under simulated downhole conditions. *Soc. Petrol. Engrs J.* **25**, 143–156.

Glowka, D. A. & Stone, C. M. 1986. Effects of thermal and mechanical loading on PDC bit life. *Soc. Petrol. Engrs Drilling Engng* **1**, 201–214.

Graves, W. 1986. Bit-generated rock textures and their effect on evaluation of lithology, porosity, and shows in drill-cutting samples. *Bull. Am. Ass. Petrol. Geol.* **70**, 1129–1135.

Gray, A. & Mathews, G. B. 1952. *A Treatise on Bessel Functions and Their Application to Physics* (2nd edn). Macmillan, London.

Hibbs, L. E., Jr, & Wentorf, R. H., Jr. Borazon and diamond compact tools. *High Temperatures–High Pressures* **6**, 409–413.

Hibbs, L. E., Jr. & Lee, M. 1978. Some aspects of the wear of polycrystalline diamond tools in rock removal processes. *Wear* **46**, 141–147.

Jaeger, J. C. 1942. Moving sources of heat and the temperatures at sliding contacts. *Proc. R. Soc. N.S.W.* **76**, 203–224.

Keller, W. S. & Crow, M. L. 1983. Where and how not to run PDC bits. Paper 11387, 1983 International Association of Drilling Contractors/Society of Petroleum Engineers Drilling Conference, New Orleans, Louisiana.

Offenbacher, L. A., McDermaid, J. D. & Patterson, C. R. 1983. PDC bits find application in Oklahoma drilling. Paper 11389, 1983 International Association of Drilling Contractors/Society of Petroleum Engineers Drilling Conference, New Orleans, Louisiana.

OGJ 1982. Contractor uses diamond shear bits in air drilling. *Oil & Gas J.* **80**, 164–172.

Ortega, A. & Glowka, D. A. 1984. Frictional heating and convective cooling of polycrystalline diamond drag tools during rock cutting. *Soc. Petrol. Engrs J.* **24**, 121–128.

Melaugh, J. F. & Saltzer, J. A. 1981. Development of a predictive model for drilling pressurized shale with Stratapax blank bits. ASME Energy Technology Conference, Houston, Texas.

Rabinowicz, E. 1965. *Friction and Wear of Materials*. John Wiley, New York.

Slack, J. B. 1981. Polycrystalline diamond bits. *Drilling* **43**, 166–170.

Sobolev, V. S. & Dobretsov, N. L. 1972. Experimental data as evidence of metamorphic conditions. In: *The Facies of Metamorphism* (edited by Sobolev, V. S.). Department of Geology, Australian National University, Canberra, 52–97.

Spray, J. G. 1989. Private communication, University of New Brunswick, Fredericton, Canada.

Swenson, D. V. 1983. Modelling and analysis of drag bit cutting. Report SAND83-0278, Sandia National Laboratories, Albuquerque, New Mexico.

Taylor, J. C. M. 1983. Bit-metamorphism, illustrated by lithologic data from German North Sea Wells. *Geologie Mijnb.* **62**, 211–219.

Tutluoglu, L. & Hood, M. 1985. Rock cutting with polycrystalline diamond compact bits and moderate-pressure water jets. *Soc. Petrol. Engrs* AIME Paper 13544.

van Proyen, J., Juergens, R. & Gilbert, H. E. 1982. Recent field results with new bits. *J. Petrol. Tech.* **34**, 1938–1946.

Zeuch, D. H. & Finger, J. T. 1985. Rock breakage mechanisms with a PDC cutter. Paper 14219, 60th Annual Technology Conference and Exhibition of the Society of Petroleum Engineers, Las Vegas, Nevada.

APPENDIX

Calculation of frictional temperature rise in the rock

The procedure for calculating the dimensionless temperature field in the rock beneath a drag cutter is presented below.

1. Specify y, z, L, χ and V (for a cutter on a rotary bit, $V = 2\pi RN$).
2. $Y = \frac{Vy}{2\chi}$; $Z = \frac{Vz}{2\chi}$; $D = \frac{VL}{4\chi}$.
3. $u_1 = Y - D = D\left(\frac{2y}{L} - 1\right)$; $u_2 = Y + D = D\left(\frac{2y}{L} + 1\right)$.
4. $\Delta u = (u_2 - u_1)/n$, where $n = 1000$ gives accurate results.
5. $u = u_1 + \frac{\Delta u}{2}$; $T_D = 0$.
6. $\zeta = \sqrt{Z^2 + u^2}$.
7. Calculate $K_0(\zeta)$ either by: (1) interpolation from tables such as Gray & Mathews (1952), Table X, pp. 313–314; or (2) using equation (13h) and a numerical integration technique employing the dummy variable ξ. (Note that the term inside the integral in equation 13h goes to near-zero for values of ξ larger and smaller than 1.)
8. $T_D = T_D + \exp(-u)K_0\Delta u$.
9. $u = u + \Delta u$.
10. If $u < u_2$, go to step 6.

This procedure was used to calculate the dimensionless temperature, T_D, for cutter 1 after the bit has drilled 20 m. The pertinent parameter values for this cutter at this point in this analysis were: $A_w = 0.065$ cm^2; $L = 0.176$ cm; and $R = 0.889$ cm.